NANO LETTERS

pubs.acs.org/NanoLett

High-Performance Carbon Nanotube Light-Emitting Diodes with Asymmetric Contacts

Sheng Wang,*,† Qingsheng Zeng,† Leijing Yang,† Zhiyong Zhang,† Zhenxing Wang,† Tian Pei,† Li Ding,† Xuelei Liang,† Min Gao,† Yan Li,‡ and Lian-Mao Peng*,†

†Key Laboratory for the Physics and Chemistry of Nanodevices and Department of Electronics, Peking University, Beijing 100871, China, and ‡Key Laboratory for the Physics and Chemistry of Nanodevices and College of Chemistry and Molecular Engineering, Peking University, Beijing 100871, China

ABSTRACT Electroluminescence (EL) measurements are carried out on a two-terminal carbon nanotube (CNT) based light-emitting diode (LED). This two-terminal device is composed of an asymmetrically contacted semiconducting single-walled carbon nanotube (SWCNT). On the one end the SWCNT is contacted with Sc and on the other end with Pd. At large forward bias, with the Sc contact being grounded, electrons can be injected barrier-free into the conduction band of the SWCNT from the Sc contact and holes be injected into the valence band from the Pd electrode. The injected electrons and holes recombine radiatively in the SWCNT channel yielding a narrowly peaked emission peak with a full width at half-maximum of about 30 meV. Detailed EL spectroscopy measurements show that the emission is excitons dominated process, showing little overlap with that associated with the continuum states. The performance of the LED is compared with that based on a three-terminal field-effect transistor (FET) that is fabricated on the same SWCNT. The conversion efficiency of the two-terminal diode is shown to be more than three times higher than that of the FET based device, and the emission peak of the LED is much narrower and operation voltage is lower.

KEYWORDS Carbon nanotube, LED, CNT diode, FET, EL

A high efficient light-emitting diode (LED) has been one of the top priority targets for the development of carbon-based optoelectronics.[1−3] While extensive investigations have been carried out on carbon nanotube (CNT) based diodes,[4−8] only few investigations on the characteristics of CNT based LEDs have been reported.[1,3] The most successful CNT based light emitters are those field effect transistor (FET) based emitters.[9,10] The FET can be either ambipolar type, where at large bias and under suitable gate voltage electrons and holes can be injected simultaneously into the CNT channel and recombine to yield electroluminescence (EL),[9] or the FET can be unipolar, where only one type of carrier (e.g., holes for p-type FET) is injected into the CNT.[10] At large bias a strong electric field may be generated around local defects to induce impact excitations or ionizations, generating electron−hole pairs and subsequently giving rise to EL.[10] More recently, an extremely efficient p−n diode based on CNT was demonstrated.[3] However, this device relies on the use of at least three independent biases to the diode,[5] to generate electron-rich (n-) and hole-rich (p-) regions, and this increases the complexity in the design and fabrication of integrated nanoelectronic and optoelectronic circuits.

Interest in CNT based photoelectronics stems from the possibility of producing low-cost, high-efficiency, lightweight, and flexible devices which can be used in integrated multifunctional photonic circuits.[1] In recent years, extensive photoluminescence (PL) studies on carbon nanotubes have demonstrated the dominant role of many-body interactions in the excited states of this one-dimensional (1D) system.[11−14] The optical properties of semiconducting single-walled CNTs (SWCNTs) are governed by excitons because of the large exciton binding energy. Experimentally it has been shown that for a (6,5) SWCNT with a diameter of 0.76 nm the exciton binding energy is roughly 0.42 eV, which is a significant fraction of the band gap of the CNT.[13] The many significant advancements in CNT based nanoelectronics have greatly prompted the used of CNTs as light-emitting devices, such as those based on semiconducting CNTs via ambipolar and unipolar FETs,[15−17] or alternatively on metallic SWCNTs via blackbody irradiation.[18,19] The EL spectra resulting from blackbody irradiation are, however, much broader than that from excitonic states, and the conversion efficiency is much lower.

Existing three-terminal EL devices may be generally classified into two types, those based on ambipolar FETs[9] and those based on unipolar FETs.[10] The ambipolar FET based devices require large source−drain and gate biases to allow for significant amounts of electrons and holes being injected simultaneously via tunneling from the end contacts into the CNT channel.[15−17] On the other hand, EL excitations

* To whom correspondence should be addressed, shengwang@pku.edu.cn (SW) and lmpeng@pku.edu.cn (LMP).

Received for review: 04/29/2010
Published on Web: 11/30/2010

DOI: 10.1021/nl101513z | *Nano Lett.* **2011,** *11,* 23–29

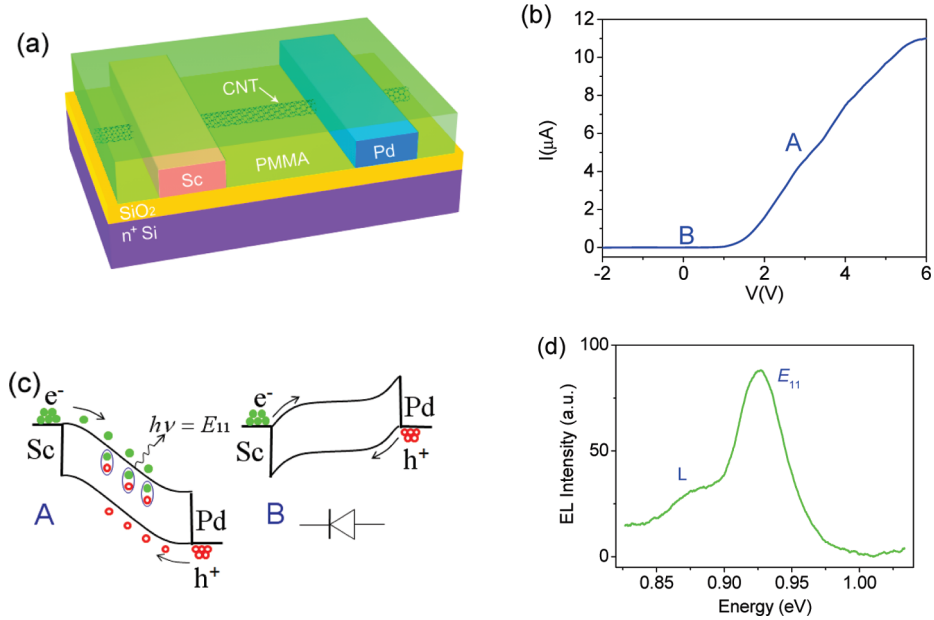

FIGURE 1. Structure and characteristics of a CNT light-emitting diode. (a) Schematic diagram illustrating the structure of an asymmetrically contacted CNT device. In all electric measurements, the Sc contact was grounded and the bias V was applied on the Pd contact. (b) Experimental $I-V$ characteristics of the CNT diode (device 1 with a channel length $\sim 1\ \mu$m) showing a typical rectifying behavior of a diode. (c) Band diagrams which correspond to the two representative points A and B of (b). At point A, the diode is forward biased, while at point B the diode is zero or slightly reversed biased. (d) EL spectrum of the diode when operated at large forward bias with a large diode current $I = 7.5\ \mu$A.

via impact ionization may be generated in a unipolar FET. At large bias the carriers can acquire enough energy to induce impact excitation and ionization at defect sites where electric field varies rapidly.[10] The use of large bias and therefore strong electric field in these devices inevitably mixes the excitonic states with that of the band-to-band continuum which leads to spectral weight transfer from the excitonic peak to the continuum and therefore yields a much broader EL spectrum.[10,15−17] EL from network CNTs has also been investigated in FET geometry using CNT films or arrays of aligned CNTs.[20−23] But excitation mechanisms in these devices are more complicated due to the additional interactions between CNTs. Furthermore, the injection efficiency of carriers in these devices is also much lower than that in single CNT based devices.

The two-terminal p−n junction LEDs are the basic building block of modern optoelectronics systems.[24] These devices have some significant advantages as light sources, including lower power consumption, easy to fabricate, lower cost, and relative simpler drive circuitry. Very recently, a CNT based light-emitting p−n diode was developed by an IBM group using the electrostatic doping technique.[3,5] But the structure of this p−n diode is very complex requiring multiple drive voltages, to bias the diode and to form electron (n-) and hole (p-) rich regions. Unlike the usual LED,[24] which is a forward biased p−n junction and carriers are supplied to the diode mainly via thermal excitations, the IBM CNT p−n diode operates at a small bias and carriers are injected into the CNT channel via tunneling rather than via thermal excitations. This operation mode greatly limits the current that may be utilized for light emission.

In an early paper we reported the electrical performance of a doping-free CNT CMOS inverter-based bipolar diode,[7] and here we show that this CNT diode may also be used as an effective LED. All experimental results reported in this Letter were obtained from devices fabricated on the same semiconducting SWCNT (results based on another CNT are shown in Figure S1 in the Supporting Information). The SWCNT was grown by a chemical vapor deposition (CVD) method on a heavily n-doped silicon substrate which was covered with a layer of insulating SiO_2 (100 nm).[25] The diameter of the SWCNT was measured by atomic force microscopy (AFM) and characterized by resonance Raman measurements. In these experiments, an excitation laser with $\lambda = 785$ nm was used, and a radial breathing mode (RBM) peak centered at $\Omega_{RBM} \approx 217\ cm^{-1}$ was observed (see Figure S2 in the Supporting Information). The diameter of this CNT is determined to be 1.14 nm using the relation $d = 248/\Omega_{RBM}$,[11,26] and this is consistent with the E_{1u} excitonic peak observed in our EL spectra and also with PL excitation spectroscopy (Kataura plot) data for a CNT with a diameter of 1.14 nm.[11,14,26] Both CNT diodes and FETs discussed in this Letter were fabricated using 60 nm Sc and Pd contacts.[7] The device structure of the carbon nanotube diode is shown in Figure 1a, and typically the device is fully covered with a 180 nm thin film poly(methyl methacrylate) (PMMA) to improve its long time stability. All electrical transport measurements were carried out with Keithley 4200 semiconductor analyzer at room temperature. EL measurements were carried out with a 300 line/mm grating and a liquid nitrogen cooled InGaAs detector linear array 512 × 1 pixels (detects $E > 0.8$ eV) (Jobin Yvon/Horiba company), and all EL spectra

DOI: 10.1021/nl101513z | *Nano Lett.* **2011,** *11,* 23–29

were collected using a microscope objective (50×) lens. A typical integration time of 60 s was used for collecting the spectra. All EL measurements were performed in the atmosphere. Raman spectra of the SWCNT were obtained using an excitation laser of 785 nm and a standard microscope objective (100×) lens.

The structure of our CNT diode is shown in Figure 1a. This diode is composed of an intrinsic (or no intentionally doped) CNT channel of about 1 μm, which is asymmetrically contacted on the one terminal by Sc and on the other terminal by Pd. Earlier studies have shown that Sc can make a perfect Ohmic contact with the conduction band of the CNT[27] while Pd makes perfect Ohmic contact with the valence band of the CNT.[28] The asymmetrically contacted CNT may therefore be regarded as a contact doped p−n junction, and the current−voltage (I−V) characteristic measured from this device (Figure 1b) shows that indeed this device behaves as a diode.[7,8] At large bias (e.g., at point A in Figure 1b) electrons are injected barrier-freely from the Sc contact into the conduction band and holes are injected into the valence band from the Pd electrode. When these injected electrons radiatively combine with injected holes in the CNT channel, photons are emitted as schematically shown in Figure 1c. The emitted photon energy distribution or EL spectrum (Figure 1d) shows a clear emission peak at 0.925 eV. At zero or low reverse bias (e.g., at point B in Figure 1b) both electrons at the Sc contact and holes at the Pd contact are subjected to a large potential barrier of the order of the band gap of the CNT (Figure 1c) and the total current is reduced to a negligible value. However, for large reverse bias the potential barrier near the contacts may be reduced significantly to allow efficient tunneling leading to large leakage current.

The EL spectrum of Figure 1d shows clearly an emission peak at 0.925 eV which may well be fitted using a Gaussian to yield a peak with a full width at half-maximum (fwhm) of about 40 meV. This emission peak may be identified as that resulting from the excitonic E_{1u} state of a (12,4) SWCNT with a diameter of 1.14 nm.[14] Another weaker EL peak (marked as L in Figure 1d) is also visible. This emission peak did not result from another CNT, because only one tube is employed in this work. In addition, this single tube may be identified as a SWCNT because it has a breakdown current of about 22 μA which is typical for a single SWCNT with a channel length ~1 μm and is much smaller than that of a multiwalled CNT or CNT bundle.[28] The emission peak marked by L in Figure 1d is very similar to that observed by Mueller et al.[3] and may be attributed to have resulted from weakly localized excitons which might be associated with defects of CNT or trapping charges near dielectric surfaces.[2,29]

The EL performance of the CNT diode is current dependent. Figure 2a shows the infrared emission spectra of another CNT diode (device 2) which was fabricated on the same CNT as device 1. The emission peak at about 0.925 eV is observed in all EL spectra taken from this device, and

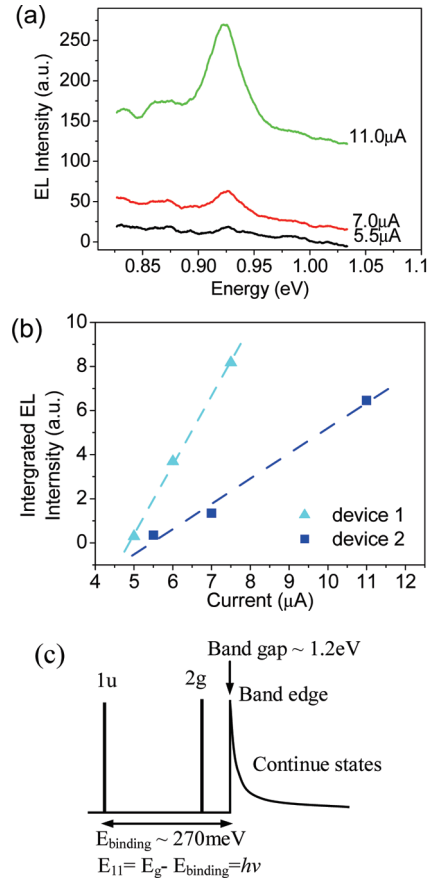

FIGURE 2. Current-dependent EL spectrum and intensity. (a) EL spectra obtained for currents between 5.5 and 11 μA for device 2 (fabricated on the same SWCNT as device 1, see Figure 1). The three EL spectra correspond respectively to V = 2, 2.5, and 4.5 V. (b) Integrated infrared emission intensity as a function of current for device 1 and device 2. (c) Schematic representation of electronic states associated with a (12,4) semiconducting SWCNT with d = 1.14 nm. The states below the band edge are bound excitonic states.

the EL intensity is seen to increase with increasing current (Figure 2b). It should be noted that for this device the fwhm of this emission peak at 0.925 eV also increases with increasing current or bias, being 26 meV for V = 2.5 V and 33 meV for V = 4.5 V respectively. This value is very close to what is observed in room temperature PL spectra, i.e., about 25 meV,[11−13] signifying the excitonic nature of this emission. Also visible in Figure 2a are some weaker luminescence peaks toward the lower energy side of the main peak at 0.925 eV, which are similar to the L peak found in Figure 1d and might also be attributed to that resulting from localized excitons. The emission efficiency of the LED device is found to vary from device to device, as manifested in Figure 2b, suggesting that the efficiency of radiative recombination of electrons and holes in device 1 is much higher than that in device 2. This is due to the stronger nonradiative recombination in device 2, such as nonradiative recombination caused by defects or trapped charge at the interface between CNT and dielectric.

DOI: 10.1021/nl101513z | *Nano Lett.* **2011,** *11,* 23–29

The integrated EL intensity shows an excellent linear relationship with current for both devices 1 and 2 (Figure 2b). Both devices exhibit current thresholds of ~5 μA for obvious light emission. The threshold current of our diodes is approximately the same as that of FET based light emitters but is significantly higher than that of the p−n diode recently investigated by the IBM group.[3] This large threshold current difference results mainly from the fact that our diode operates in the more conventional LED mode at large forward bias, while the IBM p−n diode operates at a low bias (see Figure 1c) where the current is dominated by tunneling events instead of thermal excitations. The rate for radiative recombination is thus significantly enhanced, and the threshold current is reduced.

The observed large current threshold of ~5 μA for effective light emission to occur in a CNT also signifies the difficulty in fabricating CNT based LEDs. This is because an efficient CNT LED requires roughly an equal amount of electrons and holes being injected into the CNT channel, and at the same time few defects are present in the channel where nonradiative recombination of the injected electrons and holes occur. Conventional strategy for fabricating a LED is to form a p−n junction via chemical doping. But this procedure introduces additional nonradiative sites in the channel and is therefore highly undesirable since these sites will further reduce the very limited radiative recombination rate in a SWCNT (less than 10^{-4}/per electron−hole pair). On the other hand, any symmetrically contacted CNT device will inevitably introduce a significant Schottky barrier for either electrons (in the case of p-contacts, e.g., Pd) or holes (in the case of n-contacts, e.g., Sc or Y[30]) injection from the contacts, and the best choice that one can make is to use a contact, e.g., Ti,[9] that forms a Schottky barrier with both the conduction and valence bands of the CNT with equal height (~E_g/2), making it highly unlikely to allow for a current that is substantially higher than the threshold current at low or moderate high bias. A large gate voltage may be utilized to reduce the thickness of the Schottky barrier and thus to increase the current and improve the radiative intensity of the device.

The relationship between exciton states energies and the band gap energy (E_g) of the CNT used in our experiment is depicted in Figure 2c. The observed emission peak of Figure 2a at 0.925 eV corresponds to $E_{11} = E_g - E_{binding}$, with $E_{binding}$ being the exciton binding energy. Earlier PL and optical resonance experiments have shown that for a CNT with d ~ 1.14 nm and E_{1u} ~ 0.925 eV, the CNT can be assigned an index (12,4) and a binding energy ~270 meV.[14] Figure 2a shows clearly that the E_{11} emission peak is of a fwhm of about 33 meV (with V = 4.5 V), and this corresponds to the energy state E_{1u} that is located below the band edge with a fwhm which is much less than that of the binding energy ~270 meV. The emission peak observed here at E_{11} = 0.925 eV agrees very well with that observed in the PL experiment, ~0.925 eV.[14] In principle the excitonic binding energy also depends on the dielectric environment of the CNT.[31] But our EL spectra do not show obvious E_{11} excitonic peaks shift. This is because little difference exists in the effective dielectric environments in our experiment which was on SiO_2 (ε_{eff} ≈ 2.5, half-space), covered by PMMA (ε_{eff} ≈ 3) and that of earlier PL experiments in which CNTs were suspended in solution with ε_{eff} ≈ 3.[13,17]

While our diode can generate EL, the EL characteristic depends on gate voltage and is thus subjected to additional control via the third terminal of the otherwise two-terminal device. The gate transfer characteristics of device 2 (Figure 3a) show that the device is indeed an ambipolar FET showing either electron or hole conductance for large positive (e.g., for V_g = 5 V) or negative gate voltage (e.g., for V_g = −5 V) respectively. The diode I−V characteristics (Figure 3b) and corresponding EL (Figure 3c) depend also sensitively on gate voltage. The I−V characteristics of the device exhibit good rectifying behavior for all three gate voltages V_g = −5, 1, and 5 V. However, large negative (positive) gate voltage reduces the thickness of the potential barrier near the Sc (Pd) contact, leading to enhanced leakage current (e.g., see the black curve in Figure 3b).

The two EL spectra of Figure 3c correspond to V_g = −5 V (green curve) and +5 V (black curve). Both EL spectra show a dominating emission peak at E ~ 0.925 eV, with a narrow fwhm ~30 meV, and this peak may again be identified to result from the excitonic E_{1u} state. The effect of the gate is basically to change the injection efficiency of electrons (or holes). At large negative V_g (e.g., −5 V, see the band diagram A in Figure 3d), the majority carrier type in the CNT channel is a hole. The injected holes are accumulated near the Sc contact, which may recombine with electrons injected from the Sc contact via tunneling yielding narrowly peaked EL. On the other hand, when the gate is positively biased (e.g., with +5 V, see the band diagram B in Figure 3d), the majority carrier type in the CNT channel is an electron. The injected electrons are accumulated near the Pd contact, which may recombine with holes injected from the Pd contact via tunneling yielding narrowly peaked EL. In both cases, the EL processes are dominated by excitons formed near the electrode that controls the injection of minority carriers, and the fwhm of the EL peak is therefore of the same magnitude of ~30 meV.

As a comparison, we also fabricated a unipolar n-type FET on the same SWCNT on which devices 1 and 2 were fabricated. In Figure 4 we present the gate transfer characteristic (Figure 4a) and EL spectrum (Figure 4b) of this n-type FET. For EL measurements the source electrode was grounded, and the drain and gate electrodes were biased at 10 and −3 V, respectively. At small bias, e.g., for V_{ds} < 1 V, this n-FET device is in its off-state at V_{gs} = −3 V (see Figure 4a). But when the bias is increased significantly to V_{ds} = 10 V, the tunneling barrier for the injection of holes into the valence band of the CNT is significantly reduced near the drain electrode such that appropriate amount of

DOI: 10.1021/nl101513z | Nano Lett. 2011, 11, 23–29

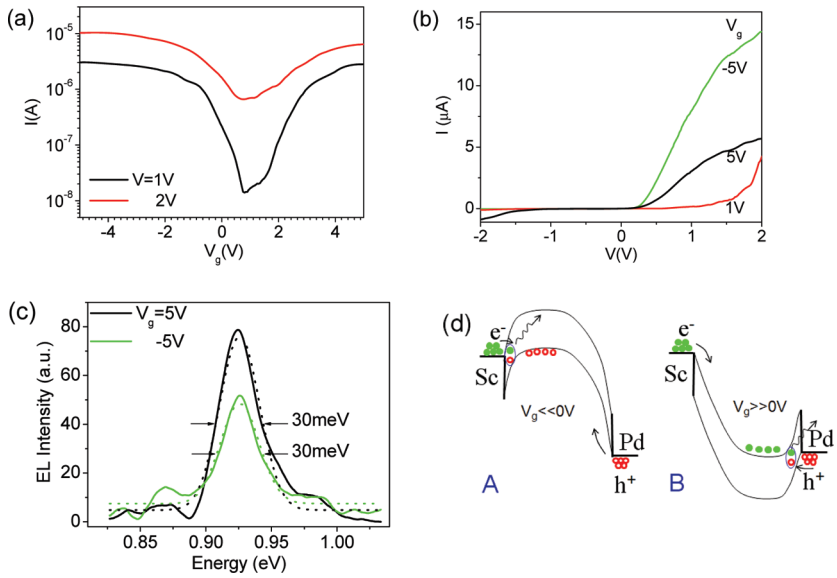

FIGURE 3. Dependence of the CNT diode (device 2) characteristics on gate bias. (a) Gate transfer characteristics ($I-V_g$) for $V = 1.0$ V (black curve) and 2.0 V (red curve), and (b) $I-V$ characteristics for $V_g = -5$, 1, 5 V. (c) EL spectra of the device under two different currents $I = 8$ μA ($V_g = 5$ V) and 12 μA ($V_g = -5$ V). Both EL spectra can be fitted well using Gaussians with the same fwhm of ~30 meV. (d) Band diagrams under different gate voltages. Points A and B correspond respectively to $V_g = -5$ V (green curve) and $V_g = 5$ V (black curve) of (c).

holes start to accumulate near the source electrode (Figure 3d) which recombine radiatively with the electrons tunneled from the source electrode resulting in a EL as shown in Figure 4b. Unlike earlier EL spectra shown in Figures 1−3, two major emission peaks may clearly be identified in Figure 4b. The stronger peak at ~0.92 eV is the same as we observed before (Figures 1−3) and may be as attributed to that resulting from the excitonic state E_{1u}, while the weaker and broader peak at ~1.06 eV may be attributed to result from the strong interaction of the excitonic state E_{1u} with higher energy excitonic and band-to-band continuous states as a result of the strong electric field (via large bias) used in this experiment. As a result of this strong interaction, the emission peak from the E_{1u} state is much broader (~150 meV) when compared with that generated from the two-terminal diode (~30 meV, see Figure 2a) we discussed earlier, and absolute emission intensity is also much lower. This is because much of the spectral weight has been transferred from the excitonic peak to the continum.[1,10,31] The presence of the large electric field also results in the accumulation of the kinetic energy for the injected carriers to result in impact excitation or ionization and therefore electron and hole pairs. Both the exciton and band gap light emissions were observed due to these impact excitations, but as was pointed out earlier the exciton emission peak is much broader due to the mixing of exciton and continuum states in the high electric field.[10] Furthermore, light emission in CNT FET (Figure 4) also proves that EL from CNT involves the same E_{11} excitonic transition as observed in devices 1 and 2.

It should be noted that the EL spectrum shown in Figure 4b was obtained in the off-state of the FET (at $V_{gs} = -3$ V) instead of in its on-state with positive V_{gs} (Figure 4a). This is because in the off-state and with a large bias $V_{ds} = 10$ V (Figure 4c), about an equal amount of electrons and holes are injected into the channel yielding highly effective radiative recombination. At small bias the minimum current I_{min} can be written as

$$I_{min} = I_e^{OFF} + I_h^{OFF} \approx 2I_e^{OFF}$$

with I_e^{OFF} being the electron current and I_h^{OFF} the hole current in the off-state. This current increases with increasing bias voltage. This is because the barrier for electron injection from the source electrode is reduced for larger V_{ds}, leading to larger I_e^{OFF}. Simultaneously the potential barrier for hole tunneling at the drain electrode is also thinned resulting in larger off-state hole current I_h^{OFF}. On the other hand, at positive gate voltage the n-FET is basically in its n-region or on-state with carriers being dominated by electrons and $I_{ds} = I_e^{ON} + I_h^{ON} \approx I_e^{ON}$, where I_e^{ON} is the on-state electron current and I_h^{ON} the on-state hole current. Since the available holes are much less than the available electrons (Figure 4d), radiative recombination is thus less effective in the on-state than in the off-state of the FET.

We now consider the EL efficiency of our diode and compare it to that of the FET based device. The external power or conversion efficiency η is defined as the ratio of the optical power output P_o to the electrical power input P_e[24]

$$\eta = (P_o/P_e) \times 100\,\%$$

where the optical power output P_o is defined as $P_o = \alpha M$, α being a system dependent constant and M being the integrated EL intensity. Since both our diodes and FET were fabricated on the same SWCNT and the same EL detector was used in all measurements, we assume that the collection

DOI: 10.1021/nl101513z | *Nano Lett.* **2011,** *11,* 23–29

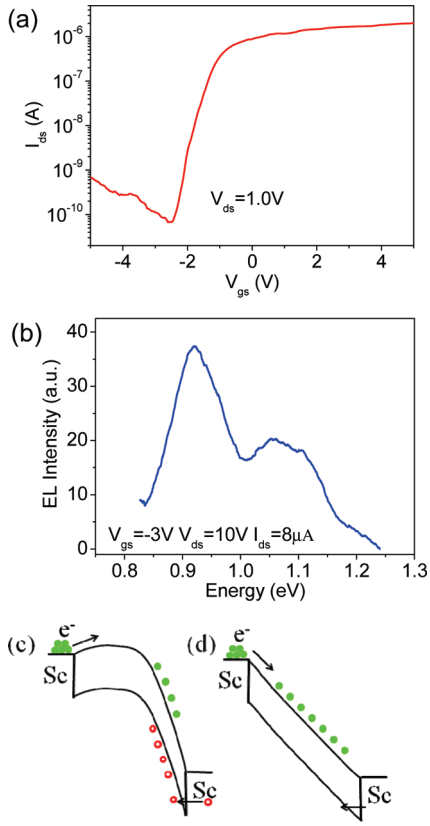

FIGURE 4. Performance and characteristics of a Sc-contacted CNT FET based emitter. (a) Gate transfer characteristic ($I_{ds}-V_{gs}$) showing a typical transport characteristic of an n-type FET. (b) EL spectrum obtained from the n-type FET. The EL measurement conditions are $V_{gs} = -3$ V and $V_{ds} = 10$ V, and the channel current $I_{ds} = 8$ μA. Band diagrams depicted for (c) $V_{gs} = -3$ V and (d) $V_{gs} = 5$ V at bias $V_{ds} = 10$ V. The n-type CNT FET was fabricated on the same semiconducting SWCNT where devices 1 and 2 were fabricated, and the conduction channel length is ~800 nm.

efficiency α is the same for all our devices. The electrical power input P_e may be calculated using $P_e = IV$. For device 1, the conversion efficiency η is estimated to be 0.093α for $I = 5$ μA (with $V = 4$ V), 0.18α for $I = 6$ μA (with $V = 5$ V), and 0.187α for $I = 7.5$ μA (with $V = 6$ V). Clearly this efficiency saturates toward 0.19α at large bias or current. On the other hand, this efficiency is estimated to be 0.055α for the FET based device with a source−drain current of 8 μA. So the light emission efficiency of our diode is about three times larger than that of the FET based device, and this may be largely attributed to the presence of the larger potential barrier and therefore higher thermal dissipation occurring in the FET based emission device.

We now consider the differences in the electrical characteristics of the asymmetric device (diode) and symmetric deive (FET). The gate transfer characteristic of an asymmetrically contacted CNT diode (Figure 3a) shows typically an ambipolar behavior; i.e., the device can be turned on or moved into its on-state either in its n-region with large positive V_{gs} or in the p-region with negative V_{gs} (Figure 5a−c). But in both n- and p-regions, the on-state current is limited

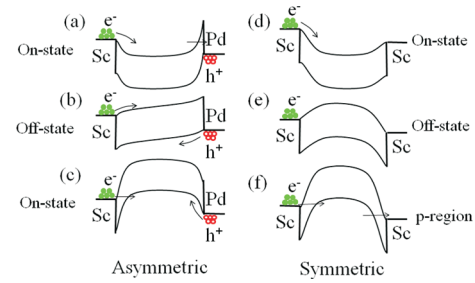

FIGURE 5. Schematic diagrams depicting the band structures of an asymmetrically contacted CNT in its (a) on-state (n-region), (b) off-state, and (c) on-state (p-region) and a symmetrically contacted n-FET in its (a) on-state (n-region), (b) off-state, and (c) p-region.

at small bias by a thin potential barrier of the order of E_g. This barrier is lowered as the bias V_{ds} is increased and becomes negative for V_{ds} larger than E_g/e. On the other hand, for a symmetrically contacted CNT device, e.g., an n-type FET, the on-state current in the n-region (Figure 5d) is much larger than that in the p-region (Figure 5f). While electrons can flow freely from the source to drain in the n-region (Figure 5d), the electron current is significantly reduced in the p-region where electrons need to tunnel through two barriers to contribute to the total current, leading to a unipolar characteristic as shown in Figure 4a.

The off-state current of a FET is mainly a thermionic current passing through the top of the potential barrier as shown in Figure 5e. This current recovers slowly as the potential barrier for electron injection being thinned for more negative V_{gs} (Figure 5f). On the other hand, the current increases much more rapidly for the asymmetrically contacted CNT in moving from off-state (Figure 5b) to on-state in the p-region (Figure 5c). Given that the on-state current for an asymmetrically contacted CNT diode is in general lower and the off-state current is higher than that of a FET, it is not surprising that the current on/off ratio for an asymmetrically contacted CNT diode is much smaller than that for a CNT FET at the same bias V_{ds}.

In summary, we have developed a high efficiency two-terminal light-emitting diode. This diode is consists of an intrinsic (or no intentionally doped) semiconducting SWCNT with a channel length of about 1 μm and a diameter of 1.14 nm, and the SWCNT is asymmetrically contacted on the one end by Sc and on the other end by Pd. Taking the Sc electrode as the ground, at large forward bias (larger than the energy bandgap of the SWCNT E_g, and in our diode it is about 1.2 eV) electrons can be injected barrier free from the Sc contact into the conduction band and holes from the Pd electrode into the valence band. These injected electrons and holes radiatively recombine yielding injection electroluminescence with a dominant emission peak centered at the lowest excitonic state energy E_{1u} and with a narrow fwhm of about 30 meV at room temperature, and total EL intensity is shown to be directly proportional to the diode current. When compared with other CNT based light emitters, our diode has the following advantages: (1) the fabrication

DOI: 10.1021/nl101513z | *Nano Lett.* **2011,** *11,* 23–29

process is doping-free and extremely cost-effective, involving only the deposition of two different (n- and p-) contacts on the semiconducting SWCNT; (2) the device is a true two-terminal diode which can be operated using a single bias; (3) only a relatively low power supply is required, which is of the same order as that associated with the CNT band gap and is typically less than 2 V; (4) the EL intensity is directly proportional to the diode current and is therefore tunable via simply changing the diode voltage or current; (5) the EL spectrum is dominated by a narrow peak of about 30 meV at room temperature that is dominated by the excitonic bound state E_{1u}, the emission peak energy can in principle be tuned by choosing SWCNT of different diameter or E_{1u}; (6) the fabrication of the diode is 100% compatible with that of the doping-free CNT CMOS process.[27] Indeed this device structure was first investigated as part of a CNT CMOS inverter, being the redundant part between a p-type FET (Pd-contacted) and n-type FET (Sc-contacted).[7] Our strategy of employing contact doping instead of chemical doping in the fabrication of CNT based CMOS and optoelectronic devices thus provides an ideal platform for a seamless integration of CNT based nanoelectronic and optoelectronic circuits.

Acknowledgment. This work was supported by the Ministry of Science and Technology of China (Grant Nos. 2011CB933001 and 2011CB933002), National Science Foundation of China (Grant Nos. No. 61071013 and 61001016), and the Fundamental Research Funds for the Central Universities.

Supporting Information Available. Figures showing the EL spectrum of a CNT based LED device and Raman spectrum of a carbon nanotube. This material is available free of charge via the Internet at http://pubs.acs.org.

REFERENCES AND NOTES

(1) Hertel, T. *Nat. Photonics* **2010**, *4*, 77–78.
(2) Avouris, P.; Freitag, M.; Perebeinos, V. *Nat. Photonics* **2008**, *2*, 341–350.
(3) Mueller, T.; Kinoshita, M.; Steiner, M.; Perebeinos, V.; Bol, A. A.; Farmer, D. B.; Avouris, P. *Nat. Nanotechnol.* **2010**, *5*, 27–31.
(4) Zhou, C.; Kong, J.; Yenilmez, E.; Dai, H. *Science* **2000**, *290*, 1552–1555.
(5) Lee, J. U.; Gipp, P. P.; Heller, C. M. *Appl. Phys. Lett.* **2004**, *85*, 145–147.
(6) Bosnick, K.; Gabor, N.; McEuen, P. *Appl. Phys. Lett.* **2006**, *89*, 163121-1:3.
(7) Wang, S.; Zhang, Z. Y.; Ding, L.; Liang, X. L.; Sun, J.; Xu, H. L.; Chen, Q.; Cui, R. L.; Li, Y.; Peng, L.-M. *Adv. Mater.* **2008**, *20*, 3258–3262.
(8) Wang, S.; Zhang, L. H.; Zhang, Z. Y.; Ding, L.; Zeng, Q. S.; Wang, Z. X.; Liang, X. L.; Gao, M.; Shen, J.; Xu, H. L.; Chen, Q.; Cui, R. L.; Li, Y.; Peng, L.-M. *J. Phys. Chem. C* **2009**, *113*, 6891–6893.
(9) Misewich, J. A.; Martel, R.; Avouris, Ph.; Tsang, J. C.; Heinze, S.; Tersoff, J. *Science* **2003**, *300*, 783–786.
(10) Chen, J.; Perebeinos, V.; Freitag, M.; Tsang, J.; Fu, Q.; Liu, J.; Avouris, P. *Science* **2005**, *310*, 1171–1174.
(11) Bachilo, S. M.; Strano, M. S.; Kittrell, C.; Hauge, R. H.; Smalley, R. E.; Weisman, R. B. *Science* **2002**, *298*, 2361–2366.
(12) O' Connell, M. J.; Bachilo, S. M.; Huffman, C. B.; Moore, V. C.; Strano, M. S.; Haroz, E. H.; Rialon, K. L.; Boul, P. J.; Noon, W. H.; Kittrell, C.; Ma, J.; Hauge, R. H.; Weisman, R. B.; Smally, R. E. *Science* **2002**, *297*, 593–596.
(13) Wang, F.; Dukovic, G.; Brus, L. E.; Heinz, T. F. *Science* **2005**, *308*, 838–841.
(14) Dukovic, G.; Wang, F.; Song, D.; Sfeir, M. Y.; Heinz, T. F.; Brus, L. E. *Nano Lett.* **2005**, *5*, 2314–2318.
(15) Freitag, M.; Perebeinos, V.; Chen, J.; Stein, A.; Tsang, J. C.; Misewich, J. A.; Martel, R.; Avouris, P. *Nano Lett.* **2004**, *4*, 1063–1066.
(16) Marty, L.; Adam, E.; Albert, L.; Doyon, R.; Ménard, D.; Martel, R. *Phys. Rev. Lett.* **2006**, *96*, 36803.
(17) Xia, F.; Steiner, M.; Lin, Y.-M.; Avouris, P. *Nat. Nanotechnol.* **2008**, *3*, 609–613.
(18) Mann, D.; Kato, Y. K.; Kinkhabwala, A.; Pop, E.; Cao, J.; Wang, X.; Zhang, L.; Wang, Q.; Guo, J.; Dai, H. J. *Nat. Nanotechnol.* **2007**, *2*, 33–38.
(19) Xie, L. M.; Farhat, H.; Son, H.; Zhang, J.; Dresselhaus, M. S.; Kong, J.; Liu, Z. F. *Nano Lett.* **2009**, *9*, 1747–1751.
(20) Adam, E.; Aguirre, C. M.; Marty, L.; St-Antoine, B. C.; Meunier, F.; Desjardins, P.; Ménard, D.; Martel, R. *Nano Lett.* **2008**, *8*, 2351–2355.
(21) Lefebvre, J.; Austing, D. G.; Finnie, P. *Phys. Status Solidi RRL* **2009**, *3*, 199–201.
(22) Engel, M.; Small, J. P.; Steiner, M.; Freitag, M.; Green, A. A.; Hersam, M. C.; Avouris, P. *ACS Nano* **2008**, *2*, 2445–2452.
(23) Zaumseil, J.; Ho, X.; Guest, J. R.; Wiederrecht, G. P.; Rogers, J. A. *ACS Nano* **2009**, *3*, 2225–2234.
(24) Bhattacharya, P. *Semiconductor optoelectronic devices*, 2nd ed.; Prentice-Hall: Englewood Cliffs, NJ, 1997.
(25) Zhou, W. W.; Han, Z. Y.; Wang, J. Y.; Zhang, Y.; Jin, Z.; Sun, X.; Zhang, Y. W.; Yan, C. H.; Li, Y. *Nano Lett.* **2006**, *6*, 2987.
(26) Weisman, R. B.; Bachilo, S. M. *Nano Lett.* **2003**, *3*, 1235–1238.
(27) Zhang, Z. Y.; Liang, X. L.; Wang, S.; Yao, K.; Hu, Y. F.; Zhu, Y. Z.; Chen, Q.; Zhou, W. W.; Li, Y.; Yao, Y. G.; Zhang, J.; Peng, L.-M. *Nano Lett.* **2007**, *7*, 3603–3607.
(28) Javey, A.; Guo, J.; Wang, Q.; Lundstrom, M.; Dai, H. J. *Nature* **2003**, *424*, 654–657.
(29) Kiowski, O.; Arnold, K.; Lebedkin, S.; Hennrich, F.; Kappes, M. *Phys. Rev. Lett.* **2007**, *99*, 237402.
(30) Ding, L.; Wang, S.; Zhang, Z. Y.; Zeng, Q. S.; Wang, Z. X.; Pei, T.; Yang, L. J.; Liang, X. L.; Shen, J.; Chen, Q.; Cui, R. L.; Li, Y.; Peng, L.-M. *Nano Lett.* **2009**, *9*, 4209–4214.
(31) Perebeinos, V.; Tersoff, J.; Avouris, P. *Phys. Rev. Lett.* **2004**, *92*, 257402–4.
(32) Piper, W. W.; Williams, F. E. *Phys. Rev.* **1958**, *98*, 1809–1813.

DOI: 10.1021/nl101513z | *Nano Lett.* **2011,** *11,* 23–29